Materials Science & Engineering C 98 (2019) 969–981

Contents lists available at ScienceDirect

Materials Science & Engineering C

journal homepage: www.elsevier.com/locate/msec

Ultrasound sonication prior to electrospinning tailors silk fibroin/PEO membranes for periodontal regeneration

Ricardo Serôdio[a,b], Sónia L. Schickert[b], Ana R. Costa-Pinto[a], Juliana R. Dias[c,d], Pedro L. Granja[c,d], Fang Yang[b], Ana L. Oliveira[a,*]

[a] CBQF - Centro de Biotecnologia e Química Fina, Laboratório Associado, Escola Superior de Biotecnologia, Universidade Católica Portuguesa, Porto, Portugal
[b] Department of Regenerative Biomaterials, Radboud University Medical Center, Nijmegen, the Netherlands
[c] i3s – Instituto de Investigação e Inovação em Saúde, Universidade do Porto, Portugal
[d] CDRsp – Centro para o Desenvolvimento Rápido e Sustentado do Produto, Instituto Politécnico de Leiria, Portugal

ARTICLE INFO

Keywords:
Silk fibroin
Poly(ethylene oxide) membrane
Periodontal regeneration
Electrospinning
Ultrasound sonication

ABSTRACT

In this study, silk fibroin (SF)/poly(ethylene oxide) (PEO) membranes were designed and fabricated by combining ultrasound sonication prior to electrospinning (0 to 20 min) as a strategy to physically control the rheological properties of solutions (10 to 30% w/v PEO) and to improve the spinnability of the system. PEO has proved to be essential as a co-spinning agent to assure good membrane reproducibility and enough flexibility for clinical manipulation.

The rheological tests indicated that sonication greatly increased the viscosity of SF/PEO solutions and further enhanced the quality of the produced electrospun fibers with consequent improved mechanical properties in dry and wet conditions. By tuning the viscosity of the solutions using a simple sonication step prior to electrospinning, it was possible to induce water stability in the as-electrospun matrix, as demonstrated by infra-red spectroscopy. This reduced complexity in the process since it was not necessary to concentrate silk prior to electrospinning while avoiding the use of toxic solvents to perform a post-processing stabilization treatment which usually causes dimensional changes to the SF materials.

Sonication pre-treatment allowed for minimizing the amount of synthetic polymer used to achieve the desirable mechanical properties (with the modulus ranging between 90 and 170 MPa), while avoiding a further water stabilization treatment. It also had a positive impact in the in vitro cell behavior of human primary periodontal ligament cells (hPDLs), resulting in a marked increase in cell proliferation. The present developed work constitutes a step forward towards simplicity and a better fabrication control of viable electrospun SF-based membranes for periodontal regeneration.

1. Introduction

Periodontal disease is responsible for the decay and loss of the periodontal structures in adults being one of the most common oral diseases involving destruction of the tooth-supporting apparatus [1]. The development of this disease is usually associated with the accumulation of an organized bacterial biofilm near the tooth also known by dental plaque [1], which ultimately can cause the deterioration of the collagen and consequently the periodontal ligaments [2]. As a result, a phenomena known as “periodontal pocket” occurs [2], due to the resorption of the alveolar bone and the relocation of the gingiva along the tooth surface. A “National Health and Nutrition Examination Survey” study carried in the United States, estimated that between 2009 and 2012, 46% adults aged 30 and over suffered from periodontitis [3]. This number increases up to 70.1% in adults with 65 or older.

Regenerative periodontal therapy comprises techniques specially designed to fully restore the architecture and function of the affected area. However, only tissue repair has been achieved [4]. Thereby, other surgical approaches have gained recognition in the attempt to restore the lost periodontal tissues [4], promoting tissue integration, including formation of new periodontal ligament with its collagen fibers functionally oriented to the newly formed cement and alveolar bone [5]. Based on this idea, the concept of guided tissue regeneration (GTR) was developed Nyman et al. in 1982 [6]. The GTR technique relies on the

* Corresponding author at: CBQF – Centro de Biotecnologia e Química Fina, Escola Superior de Biotecnologia, Universidade Católica Portuguesa, Porto, Rua Arquiteto Lobão Vital 172, 4200-374 Porto, Portugal.
E-mail address: aloliveira@porto.ucp.pt (A.L. Oliveira).

https://doi.org/10.1016/j.msec.2019.01.055
Received 8 June 2018; Received in revised form 7 December 2018; Accepted 12 January 2019
Available online 15 January 2019
0928-4931/

use of an occlusive membrane, which will be applied over the periodontal defect, thus promoting wound repopulation by PDL cells and inducing periodontal tissue regeneration [4,7].

Currently, a wide diversity of structures (carriers, grafts, scaffolds and membranes) has been described to be applied in periodontal defects, promoting the regeneration of periodontal tissue. These include autogenic, allogenic and xenogeneic grafts [8], natural component membranes [9,10] or synthetic carriers [8]. Regardless of the used material, it is important to understand that the key parameters of these structures need to be assured for a bidirectional cell-membrane interaction [8]. Apart from the biocompatibility requirements of the material with the surrounding structures of periodontal ligament, the provided structure also needs to be able to isolate the wounded space, thus excluding the invasion of undesirable cells [7,9,10]. Polytetrafluoroethylene (PTFE) non-absorbable membranes are a well-recognized standard in clinical use [11]. However, to exclude a second surgical procedure, the demand for absorbable biomaterials increased and several bioabsorbable membranes have been proposed [12]. Synthetic polyglycolic acid (PGA) and its copolymer (PLGA) [13], polylactic acid (PLA) [13], natural chitosan [14,15], gelatin [16] and collagen [17], are just some of the most commonly used.

Silk fibroin is a natural polymer with remarkable mechanical properties, proven biocompatibility, oxygen and water vapor permeability, proteolytic degradability and minimal inflammatory reaction, besides being easy to process at a low cost [18,19]. Taking into account these unique properties, its applicability in several biomedical fields is being investigated, including: hydrogels, nano-/microfibers, membranes, nanospheres and coatings which can support the repair and/or regeneration of skin [20], bone [21] and cartilage [22], vascular [23] or neural [24] tissues. These structures can be directly used as implants, scaffolds for tissue engineering [24] or vehicles for drug release [25].

Due to its natural ability to be spun [26], SF is particularly attractive for the production of nanofibrillar structures resembling the collagenous extra-cellular matrix (ECM), namely by electrospinning technology [27,28]. In this process, polymer concentration plays an important role on the resulting solution viscosity, which in turn reveals to be critical to the overall effectiveness of the electrospinning process and quality of the fibers [28]. Water-based silk solutions have been successfully electrospun [29,30]. However the concentrations necessary to achieve the adequate viscosity for the formation of stable fibers are relatively high, as reported for instances in the work of Wang et al. [29] in which non-less than 17% (w/v) of SF in solution was necessary to ensure the production of viable electrospun mats. However, increasing the concentration of SF-based stock solutions results in several stability problems due to its ability to self-assemble into insoluble β-sheet conformation. This leads to the conversion into a gel which is not able to be spun [31,32]. Also, the produced mats tend to be brittle, limiting its application as a flexible membrane [32]. To blend SF with polymeric additives has been therefore, a common practice. Poly(ethylene oxide) (PEO) has been used to increase the viscosity in low-concentrated SF solutions [32–34]. However, the presence of PEO was found to have a negative impact on the biocompatibility of these materials [35]. Thus, there is interest in reducing this polymer blending dependence while maintaining the fiber quality and stability of the SF matrices.

Ultrasonic treatment has been used as a strategy to tailor the viscosity of SF-based solutions [36,37]. This study intends to explore this possibility applied SF/PEO solutions, as a strategy to improve the electrospinnability and quality of the produced nanofiber membranes for periodontal regeneration. The morphology and mechanical properties of the electrospun membranes produced without and after several periods of sonication were characterized. Cell interaction with the produced nanofiber matrices was studied using human periodontal ligament cells through adhesion and proliferation tests.

2. Materials and methods

2.1. Materials

Bombyx mori cocoons, used as source of silk fibroin, were provided by the Portuguese Association of Parents and Friends of Mentally Disabled Citizens (APPA-CDM, Portugal). All the remaining reagents were purchased from Sigma-Aldrich, unless stated otherwise.

2.2. Preparation of silk fibroin/PEO solutions

Silk Fibroin was degummed through a previously developed procedure, as described elsewhere [38]. Briefly, the cocoons were boiled in a solution containing 0.02 M of sodium carbonate anhydrous (Na_2CO_3; ACROS ORGANICS) for 30 min, followed by a silk fibroin mesh rinse. In order to produce an aqueous silk fibroin solution (pure solution), degummed fibers were dissolved in a 9.3 M lithium bromide (LiBr) solution at 60 °C for 4 h, with a ratio of SF:LiBr of 1:4 (wt/v). The dissolved silk fibroin was dialyzed against distilled water, using a benzoylated dialysis tubing (molecular weight cut-off: 2000 Da), for 48 h to remove the salt. After dialysis, SF solution was centrifuged at 5000 rpm, as a purification step. The final concentration of SF in solution was ~7% (w/v) as determined by the wet weight methodology.

A variety of compositions of the SF/PEO aqueous blends were prepared, using a starting solution of 6% w/v PEO (Mv: 200 kg mol^{-1}). Three different SF/PEO blend formulations were prepared according to the SF/PEO weight percentage ratios: 90/10, 80/20 and 70/30. Before storage, the pH of all solutions was measured and adjusted to the ideal range, between pH of 7–8, in order to mimic the conditions found in the silkworm gland [39], with solutions of hydrochloric acid (HCl, 0.5 M) and sodium hydroxide (NaOH 0.5 M). All solutions were kept at 4 °C until further use.

2.3. Ultrasound sonication

SF/PEO blends were sonicated with a UP50H Compact ultrasonic lab homogenizer (50 W, Hielscher-Ultrasound Technology, Germany). The sonication parameters were first optimized, including operating frequency, cycle, time of sonication, type of sonotrode used and the sample volume. A 7 mm diameter sonotrode with a fixed frequency of 50 Hz and a continuous cycle was used. These tests were performed using an indirect sonication method, in which the sonotrode placed in contact with a water bath where the sample's tube was then positioned, at a submersion depth of 10 cm. This container was then placed in contact with ice in order to avoid the heating of the sample, caused by the ultrasounds. The temperature of the water bath was kept at ~20 °C. The different SF/PEO solutions were treated for the periods: 7.5, 15, 20 and 30 min. From this point further, it was noticed that the solutions went through a gelling process (qualitative observation), which made them non-viable for further electrospinning.

2.4. Electrospinning of the aqueous SF/PEO blends

SF/PEO solutions were electrospun for the fabrication of the nanofiber membranes using an electrospinning equipment (Fuence Esprayer ES-2000S, Japan). A schematic figure of the process is shown in Fig. 1.

The used electrospinning setup relied on three components. A high-voltage supplier, a capillary needle in which our polymeric solution will be inserted and a grounded collector (aluminum foil) [40–42]. The electrospinning process parameters were optimized to achieve stable and reproducible spinning, in particular the flow rate, applied voltage and the distance between the tip off the syringe (a 18 G tip was used) and the grounded collector. The optimized applied voltage was 30 kV. The optimized flow rate for all formulations was 20 μL/s, since that was the minimal value enabling fiber extrusion instead of droplet ejection. Based on previous studies, the height of the spinneret was adjusted to

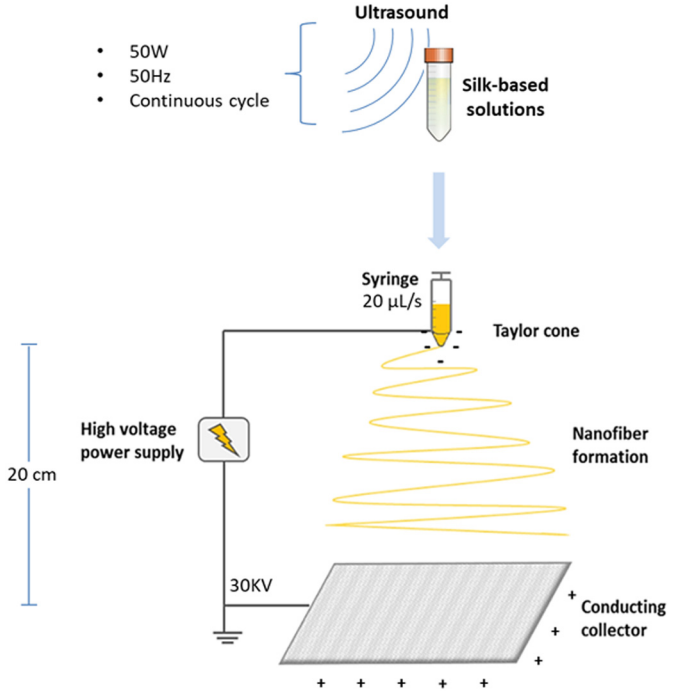

Fig. 1. Electrospinning of SF solutions with varying viscosities modulated by ultrasounds.

20 cm, because lower heights do not enable proper solvent evaporation (in this case, water) [34]. The obtained membranes were left in a fume hood for drying. Since they demonstrated water stability, no post-spinning treatment was necessary to stabilize silk II conformation, thus avoiding the use of toxic solvents.

2.5. Rheological analysis of the SF/PEO blends and pure SF solutions

The rheological tests were performed at 25 °C using a rheometer (AR 2000ex TA Instruments-USA). Before each test, samples were subjected to a constant shear rate ($\Upsilon = 10\,s^{-1}$) test was used for 100 s in order to ensure that the samples were evenly distributed (established and uniform rheological state) along the rheometer plate. After that, an oscillatory stepped flow assay, was used to access the rheological behavior of the solutions of SF/PEO with a linear increase of shear rate, from $\Upsilon = 1.000\,s^{-1}$ up to $1000\,s^{-1}$. The viscosity's "flow curves" were generated by testing the different blends over a range of shear rates (n = 3). Raw data was treated through the use of the TA Instruments TRIOS software. The values of average viscosity were then obtained by identifying the first viscosity value right after the low shear rate viscosity plateau (Linear Viscoelastic Region).

2.6. Morphological characterization – scanning electron microscopy (SEM)

SEM analysis of the SF membranes was performed using a Zeiss Sigma 300 (Oberkochen, Germany) scanning electron microscope and a Hitachi TM3000 (Tokyo, Japan) imaging software. To improve the sample's conductivity the membranes were sputtered with a 20–30 nm thick copper coating prior to imaging.

The samples were analyzed at the following magnifications, 2000×, 5000× and 10,000× with an extra high tension (EHT) of 10.00 kV. To estimate fiber diameter, "Diameter", a plugin from ImageJ, software was used. For each condition, two membranes were tested and 10 different fibers were chosen to perform 3 measurements along the length of each one. For this, SEM images with a magnification of 10,000× were used.

2.7. Fourier transform infrared spectroscopy with attenuated total reflectance (FTIR)

Fourier transform infrared spectroscopy (FTIR-ATR, PerkinElmer precisely, Spectrum 100, USA) was used to analyze the chemical structure of the produced matrices after processing. FTIR spectra were obtained in the range of wavenumber from 4000 to 450 cm^{-1} during 16 scans, with 4 cm^{-1} resolution, and region of the spectra corresponding to the fingerprint of both polymers in the blend was displayed (1800 to 800 cm^{-1}, n = 2). After obtaining the data, the spectrum was smoothed using the Spectrum software to minimize interferences.

2.8. Mechanical characterization

Mechanical properties of dry and wet SF/PEO membranes were assessed according to the ASTM D882 – 02 protocol. Uniaxial tensile test was performed using texturometer equipment (TA.XT PLUS, Texture Analyzer, UK), with a 2 N load cell. To prepare the mechanical test in the wet state, the membranes were immersed in PBS, for about 5 min before the test, to ensure that they reached full hydration. From each membrane sample 5 replicate specimens were cut with an average dimension of 3 cm length/1 cm width. The cross-section of the membrane was measured using a micrometer exactly in the center of the sample, which varied from 10 µm to 250 µm. This ensured that the deformation and failure was consistent from sample to sample and accurately representative of the material. The specimens were placed between two grips (gauge length of 100 mm) and the tensile test was performed at a 1 $mm{\cdot}s^{-1}$ speed. Ultimate Tensile Strength (UTS), Young's modulus, Stress at Break and Elongation at break were obtained from the corresponding stress/strain plots. UTS was calculated as the maximum stress that the membrane could withstand before failure; Young's modulus corresponds to the slope from the linear region of the plot; Stress at Break corresponds to the point at which the material fractures; Elongation at break corresponds to the strain (deformation) at rupture.

2.9. Water vapor permeability

The water vapor permeability method was performed according to the E96/E96M [ASTM, 2010]. In order to access the permeability of the SF/PEO electrospun membranes to water vapor, 3 circular samples with 0.016 m diameter of each formulation were cut and placed on the top of glass flask after being previous hydrated in MiliQ water for 0.5 h. The flask, filled with $8.0 \times 10^{-6}\,m^3$ of MiliQ, was then weight before and after the samples were placed on an oven at ± 35 °C for 24, 48, 72 and 168 h. The amount of lost water was calculated using the following equation:

Equation

$$WVT = \frac{G}{tA} = \left(\frac{G}{t}\right)/A \quad (1)$$

where:

In metric units:

G = weight change (from the straight line), g;

t = time, h;

A = test area (cup mouth area), m^2; and

WVT = rate of water vapor transmission, $g/h{\cdot}m^2$

An uncovered flask filled with MiliQ water was used as control.

2.10. Cytotoxicity: direct contact

The cytotoxicity of the SF/PEO membranes was assessed using human cells from the periodontal ligament (hPDLs). After signing an informed consent, PDL cells were harvested from an impacted third molar of an adult patient (18 years, female).

Cells were cultured with DMEM medium (Sigma) supplemented

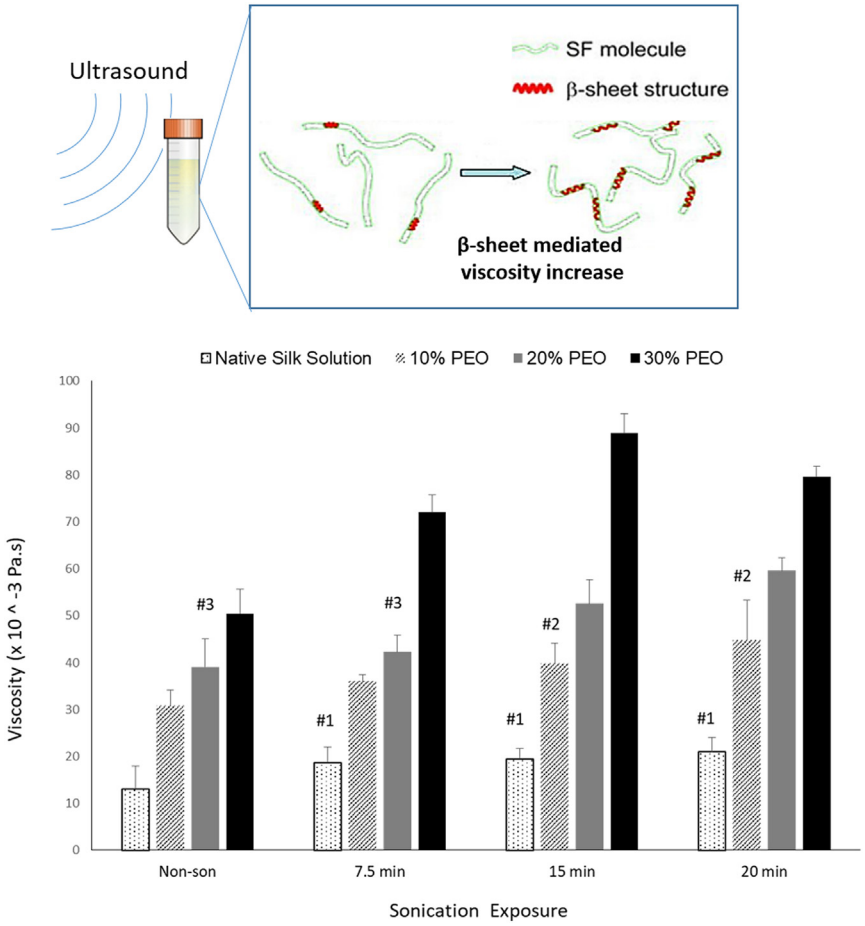

Fig. 2. Viscosity of all the tested SF and SF/PEO formulations as function of sonication time (min); (#) no significant statistical difference was observed between the samples compared ($p > 0.05$). #1 between pure silk solutions; #2 between solutions with 10% of PEO; #3 between solutions with 20% of PEO. The sketch above the plot represents SF undergoing β-sheet conformation physically induced by the ultrasounds.

with 10% fetal bovine serum (Gibco) and 1% Penicillin/Streptomycin (Gibco) under controlled conditions (37 °C, relative humidity of 95% and 5% CO_2 saturation). The medium was replaced every other day. When 90% of confluence was reached, cells were first washed with sterile PBS and detached with TrypLE Express (Gibco). In this study, hPDL cells were counted and seeded at passage number 11, in a concentration of $2{,}5 \times 10^4$ cells/membrane by means of a droplet of 30 μL, and incubated for 2 h to promote cell attachment. It has have been reported that these cells maintain its functionality (phenotype/genotype) up to passage 9 [43]. Beyond that, subsequent studies have been performed with this cell source up to passage 15 without loss of their characteristics (data to be published).

After that period, the cell-seeded membranes were transferred to new vessels and culture medium was added. At 1, 3 and 7 days the membranes were collected for different biological assays. Controls were performed with materials without cells and with cells only cultured in tissue culture polystyrene (TCPS). All assays were performed in triplicate and repeated 3 times.

For SEM analysis, samples were fixed with 2.5% glutaraldehyde solution, washed with phosphate buffered saline (PBS) and serially dehydrated with increasing concentrations of ethanol (10, 20, 30, 40, 50, 60, 70, 80, 90 and 100%), sputter-coated with a thin layer (9–12 nm) of gold/palladium (SPI Module Sputter Equipment). The specimens were further analyzed by SEM using a Quanta 400 FEG ESEM/EDAX Genesis X4M (FEI Company, USA). SEM micrographs were recorded at 15 kV with magnifications ranging between 500 and 2000 times.

Confocal microscopy imaging was performed with a laser scanning confocal microscope (LSCM) - Leica TCS SP5 (Leica, Germany). For that, at each time point, cells were fixed with formalin 10% for 15 min and further washed with PBS, and stored at 4 °C until use. At the day of the observation, cells were permeabilized using a 0,2% (v/v) Triton X100 (Sigma-Aldrich) solution for 15 min. Non-specific binding was performed with 3% bovine serum albumin (BSA; Sigma-Aldrich) for 30 min. After washing with PBS, cells were stained with phalloidin-TRITC (Sigma-Aldrich) diluted at 1:500 and incubated for 30 min. After washing with PBS, DAPI (Sigma) diluted at 1:1000 was incubated, washed with PBS and samples observed at LSCM.

Cell metabolic activity was assessed by resazurin assay. Briefly, 80 μL of resazurin (1 mg/mL) (Sigma) solution in PBS was added to each well. A blank was performed only with DMEM and resazurin. Cells were incubated for 2 h and fluorescence ($\chi_{ex/em}$ = 530/590 nm) read in a microplate reader (Synergy Mx, Biotek).

DNA concentration was determined by using a fluorimetric dsDNA quantification kit (Quant-iT™ PicoGreen®, Molecular Probes, Invitrogen, USA). Triplicates of each condition were collected at previously defined time points, washed twice with sterile PBS and transferred into Eppendorf tubes containing 1 mL of ultrapure water and stored at −80 °C. Frozen constructs were thawed and sonicated for 15 min to release intracellular DNA into the water. Prior to DNA quantification, the specimens were subjected to vortex at maximum rpm for 30 s. Per each well of a white opaque 96-well plate were added 28.8 μL of sample or standard (n = 3), 71.2 μL of PicoGreen solution and 100 μL of TE buffer. The plate was incubated for 10 min protected from light and the fluorescence was read in a microplate reader (Synergy Mx, Biotek) by using an excitation wavelength of 485/20 nm and an emission wavelength of 528/20 nm. The amount of DNA was calculated by interpolation from a standard curve prepared at dsDNA concentrations ranging from 0 to 2 μg/mL.

2.11. Statistical analysis

One-way analysis of variance was performed using IBM SPSS Statistics 22 software for the mechanical characterization and permeability tests. Statistical analyses of variance (ANOVA Two-way) analyses were performed using IBM SPSS Statistics 22 software for the rheological assays, cytotoxicity assays and SEM analysis of the electrospun fibers diameters. In this study, a 95% confidence interval was used, so the results were considered as statistically significant if the p-value was < 5%.

3. Results

3.1. Rheological analysis of the SF/PEO blends and pure SF solutions

The effect of sonication over the viscosity of the SF/PEO solutions was assessed by rheological tests. The relationship between the viscosity of the samples containing 10%, 20% and 30% of PEO, after sonication times of 7.5, 15 and 20 min is plotted in Fig. 2. Non-sonicated samples and pure SF solution (without PEO) exposed to the same sonication times were also evaluated as control groups.

The average viscosity tends to increase, as the samples are subjected to longer sonication periods, likely by the establishment of β-sheet conformation induced by the ultrasounds. As expected, the presence of PEO has also a marked influence on increasing the viscosity. In pure silk solutions the average viscosity increases from values of $\sim 13.1 \times 10^{-3}$ to $\sim 21 \times 10^{-3}$ Pa·s, before and after a sonication period of 20 min. This increase is more pronounced for higher percentages of PEO. For example, in samples with 30% PEO the viscosity increase from $\sim 50 \times 10^{-3}$ to $\sim 80 \times 10^{-3}$ Pa·s before and after a sonication period of 20 min, respectively. These results indicate that the increase of viscosity by sonication is enhanced by the presence of PEO in the structure.

After testing the viscoelastic properties of the solutions, they were processed by electrospinning. Table 1 represents a qualitative observation of each obtained solution, for the tested processing conditions.

For non-sonicated blended solutions, only those with a minimum amount of 20% of PEO and corresponding viscosity of $39.1 \pm 6 \times 10^{-3}$ Pa·s could be spun in a continuous and homogeneous membrane. Nevertheless, solutions containing 10% PEO were considered to the combined sonication and electrospinning process together with solutions containing 20%, to evaluate whether the sonication pre-treatment could enhance the processability of solutions and/or the quality of the fibers. The 30% PEO blends, when submitted to sonication, revealed levels of viscosity which did not allow for the solution to flow through the spinneret, i.e. too high for electrospinning.

3.2. Morphological characterization of the produced membranes

The effects of altering the solution properties via sonication pre-treatment while maintaining steady electrospinning process parameters, on the fiber formation, morphology, and diameter, were investigated macroscopically and by SEM, as presented in Fig. 3. The fiber diameter was calculated for each of the conditions and plotted in Fig. 4.

Fig. 3 shows SEM micrographs of the electrospan membranes. A clear influence of both PEO concentration and the sonication pre-treatment on improving the resulting quality of the produced nanofibers can be observed. Also, by analyzing Fig. 4, it is possible to understand that the fiber diameter increases with increasing concentrations of PEO and with the time of sonication pre-treatment. The membranes produced from non-sonicated solutions containing 20% and 30% of PEO presented continuous fibers with uniform diameter (Fig. 3a and b). When analyzing the correspondent fiber diameter (Fig. 4) it is possible to observe a significant increase ($p < 0.05$) with the increase of the PEO content.

When performing a sonication treatment prior to electrospinning it was possible to produce beadless and uniform nanofibers, when PEO was present at percentages of 20% (Fig. 3c and d). In this case, the effect of sonication over the fiber diameter has a significant impact ($p < 0.05$, Fig. 4), when comparing non-sonicated samples with those sonicated for a period of only 7.5 min, going from $\sim 318 \pm 18$ nm to $\sim 390 \pm 65$ nm, which is maintained after 20 min of sonication ($\sim 390 \pm 30$ nm).

When decreasing the percentage of PEO to 10% and after a sonication treatment of 15 min (Fig. 3e) it was possible to spin the solution and create a viable membrane, yet presenting irregular thickness (visual inspection of the membranes revealed thicker regions than others) and microscopically the so called “beaded-fibers” [23,44]. This irregularity did not allow for an accurate measurement of the diameter, in a reproducible manner. PEO is usually added to the SF aqueous solutions to overcome the problem of low concentration in the electrospinning process, by increasing the solution viscosity and thus avoiding the formation of droplet-like irregularities on the fibers. In our study, instead, we increased the sonication period to 20 min, which has led to the complete elimination of the bead formation (Fig. 3f) and the production of continuous fibers with a regular diameter of $\sim 388 \pm 37$ nm (Fig. 4). This diameter was in the same range of the fibers produced from solutions containing 20% PEO and sonicated for the same period ($\sim 390 \pm 30$ nm), indicating that the sonication period had a higher impact on the fiber diameter than the percentage of PEO.

3.3. Chemical analysis - Fourier transform infrared (FTIR) spectroscopy

FTIR analysis was used to study any structural changes induced by sonication on the SF/PEO electrospun membranes. Fig. 5 shows the spectra corresponding to each membrane.

Table 1
Viability of the different solutions for the electrospinning process.

Sonication treatment (minutes)	PEO (%)							
	0% (pure SF)		10%		20%		30%	
	Spinning	Comments	Spinning	Comments	Spinning	Comments	Spinning	Comments
0	X	Low viscosity	X	Possible formation of “beaded-fibers”	✓	Optimal viscosity for spinning	✓	Optimal viscosity for spinning
7.5	X	Low viscosity	X	Possible formation of “beaded-fibers”	✓	Optimal viscosity for spinning	X	High viscosity
15	X	Low viscosity	✓	Formation of “beaded-fibers”	X	Solutions with similar solution already spun	X	High viscosity
20	X	Low viscosity	✓	Optimal viscosity for spinning	✓	Optimal viscosity for spinning	X	High viscosity
30	X	High viscosity	X	High viscosity	X	High viscosity	X	High viscosity

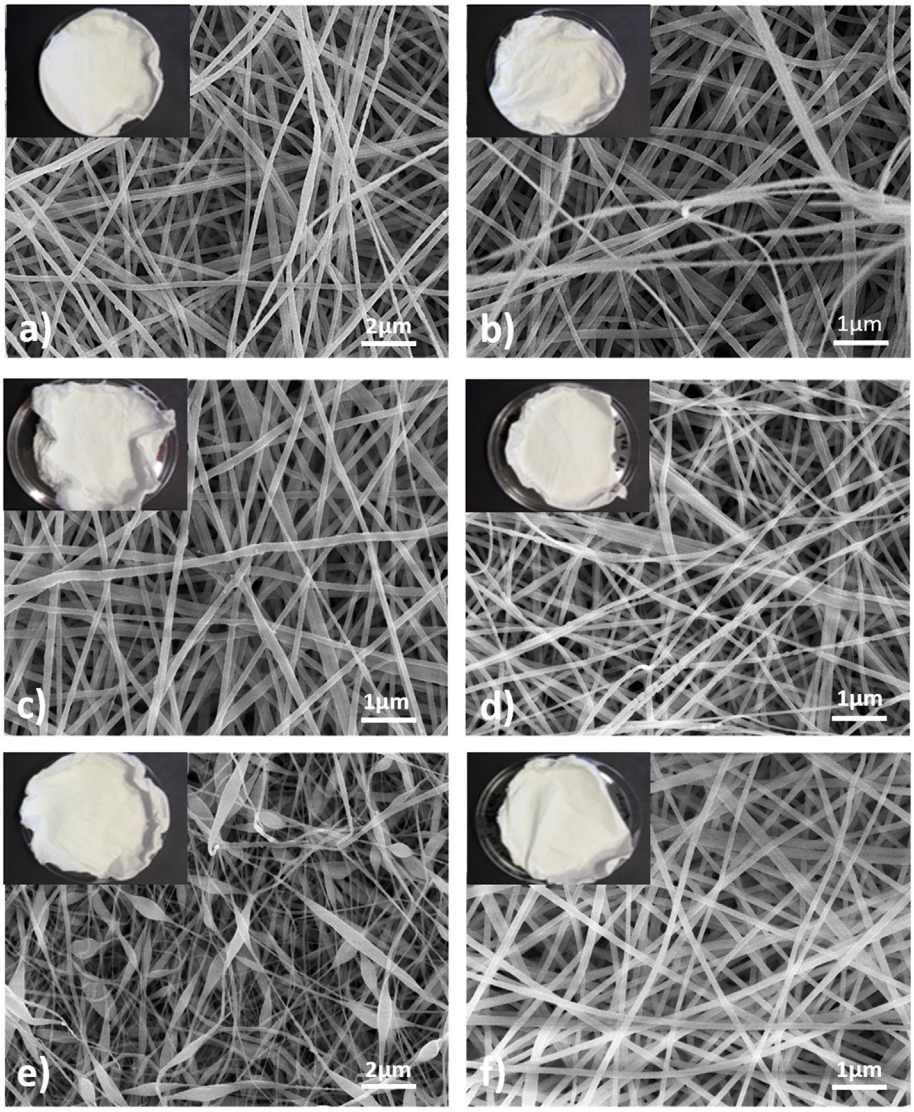

Fig. 3. Macroscopic and SEM (10,000×) images of the electrospun matrices; a) 20% PEO (Non-sonicated); b) 30% PEO (Non-sonicated); c) 20% PEO (7.5 min of sonication); d) 20% PEO (20 min of sonication); e) 10% PEO (15 min of sonication) and f) 10% PEO (20 min of sonication).

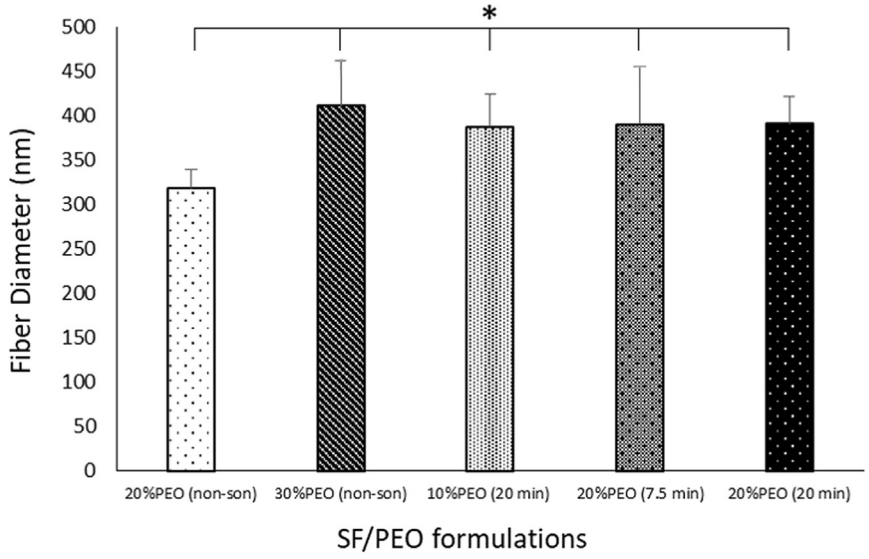

Fig. 4. Fiber diameter of the different electrospun SF/PEO formulations. The asterisk (*) means that a significant statistical difference was observed between the compared samples ($p < 0.05$).

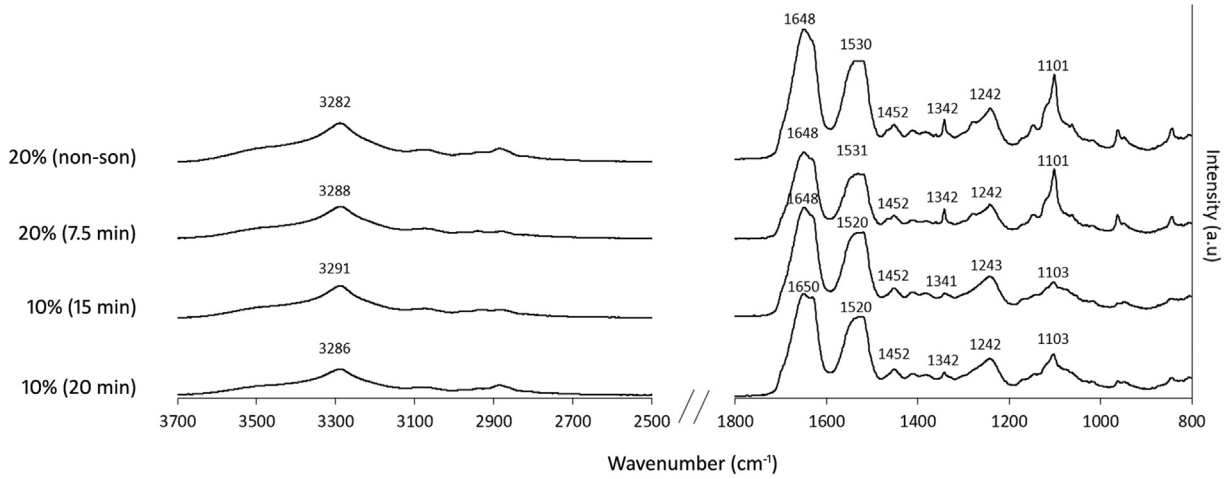

Fig. 5. a) FTIR spectra of the different SF/PEO electrospun membranes.

The spectra of all the SF/PEO membranes showed similar characteristic regions. Through the fingerprint zone (800–1800 cm^{-1}) analysis, the three major characteristic bands of SF were identified (Fig. 5), corresponding to amide I (1648 cm^{-1}) for the non-sonicated blend, which is characteristic of mainly amorphous silk conformation [45]. For the sonicated membranes, a small shoulder starts to appear at 1630 cm^{-1}, the beginning of the characteristic amide I band. The result only indicates an amide I shift to 1650 cm^{-1} upon increased ultrasound sonication exposure to 20 min.

Usually located between 1500 and 1600 cm^{-1}, the characteristic band of amide II, slightly shifts according with the PEO concentration in solution [32,45]. As indicated in the spectra and regardless of sonication periods, the 20% PEO blends show bands around 1530 cm^{-1}, however, in the case of the 10% PEO blends, the amide II band shifts to 1520 cm^{-1}. Another characteristic band of silk fibroin is located at 1238 to 1322 cm^{-1} known as the amide III [45].

The bands at 1460 and 1348 cm^{-1} are attributed to the vibrations of the CH2 - group of PEO, as well reported in the literature [46]. Likewise, the bands at 1100 and 960 cm^{-1} are due the C—O group asymmetric stretching vibrations and to C—O—H bending vibrations and the strong band near 2885 cm^{-1} is attributed to the symmetric and asymmetric C—H stretching [47]. The broad intensity band between 3200 and 3600 cm^{-1}, is attributed to O—H and N—H groups stretching vibration [47]. These bands intensify with increasing percentage of PEO.

3.4. Mechanical characterization

The mechanical tests allowed to determine the Young's Modulus, the Stress at Break, Ultimate Tensile Strength (UTS) and the Elongation at break of the electrospun membranes in dry and wet state and are presented in Fig. 6.

The performed tensile tests indicate clear differences between the mechanical properties of the produced membranes (Fig. 6a). In the dry state, the Young's Modulus (Fig. 6b) of the different samples was at least 40 times higher than in the wet state. Stress at Break also follows the same pattern, by showing that dry samples had values at least 6 times higher than those found in the wet state (Fig. 6c). The UTS values (Fig. 6d) showed a fold increase of 10 times for samples in dry state as compared to wet state, while the Elongation at Break (Fig. 6e) displays an opposite behavior, showing higher values for the wet state samples, with the exception of the non-sonicated formulation. These results indicate that the presence of water in the structure has a strong plasticizing effect in the structure of the membranes, which become more ductile.

When comparing the different processed samples in the dry state, it is worth noting that formulations with the same PEO concentration, revealed lower Young's Modulus values for longer sonication periods; 10% (15 min) and 10% (20 min) showed 166 MPa and 104 MPa respectively; whereas the 20% (non-sonicated) and 20% (7.5 min) showed 134 MPa and 90 MPa, respectively. The Stress at Break, besides increasing with higher concentrations of PEO also increased with sonication for samples with less amount of PEO, while for the materials with 20% the values were not statistically different ($p > 0.05$). Regarding the UTS results for the dry samples it is possible to note that these were affected by the sonication treatment ($p < 0.05$), since for samples containing only 10% PEO, the UTS increases from 1.19 MPa to 1.80 MPa with increasing time of sonication from 15 to 20 min. For samples with 20% there is also an increase from 2.58 MPa to 2.84 MPa with an increase of sonication exposure from 0 to 7.5 min. These UTS results are in accordance with the previously reported in the literature for this system by Suzuki et al. [48]. In this study the values of UTS were around 1–2 MPa, in the order of those achieved herein for non-treated silk membranes in dry state, 2.74 MPa. In the wet state, the elongation at break increases with sonication time for both formulations and tends to be higher with increasing percentage of PEO.

Overall, the mechanical characterization, in particular of the wet state samples, was useful to understand that increasing sonication periods does not particularly affect the Young Modulus, the Stress at Break and the UTS. On the contrary there is a strong effect in the elongation capacity of the materials, which increases with increasing sonication periods.

3.5. Permeability tests - water vapor permeability assay

The ability of the membrane to permeate biomolecules and fluids when applied to the periodontal defect can allow for gaining some insights on its suitability in a wound healing application. This was studied by permeability assays and the results are disclosed in the Fig. 7, which relates the water vapor transmission rate, along the different tested time points.

As presented, the permeability between membranes up to 7 days was very similar between all four formulations, indicating that the mass transport is not significantly altered with increasing time of sonication or with increasing percentage of PEO. Water vapor permeability is strongly dependent on the water diffusion coefficient and solubility [49]. Therefore, it becomes important to correlate the obtained values with the ability of the material to be permeable to water and biomolecules, while acting as a barrier to PDL cells.

3.6. Cytotoxicity: direct contact

Cell morphology and the interaction between the hPDLs and the

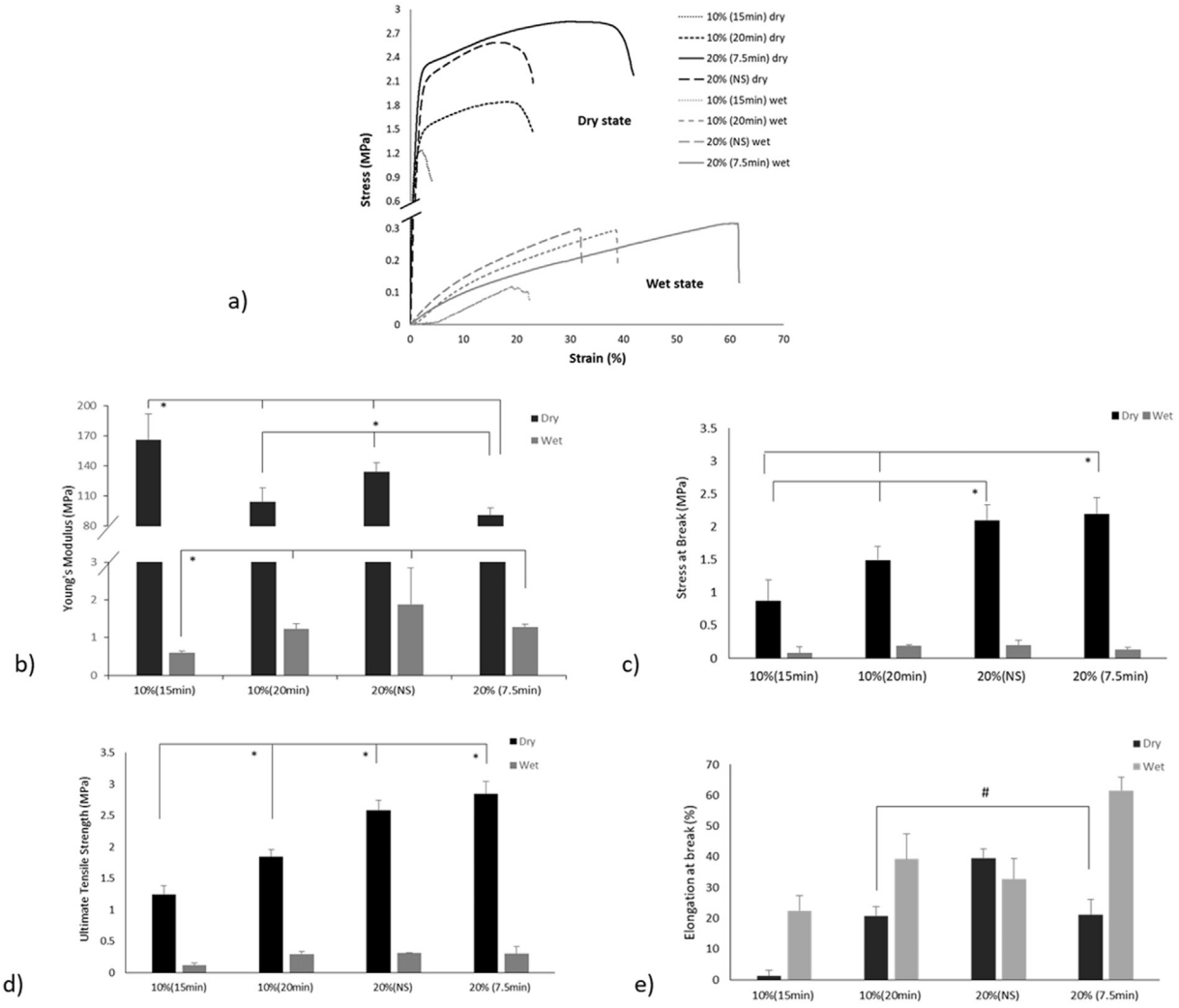

Fig. 6. Mechanical behavior of SF/PEO membranes at dry and wet states: (a) Stress-strain curves; (b) Young's Modulus; (c) Stress at Break; (d) Ultimate Tensile Strength (UTS); (e) Elongation at break. (*) means that a significant statistical difference was found between the compared samples ($p < 0.05$). (#) means that no significant statistical difference was found between the compared samples ($p > 0.05$).

silk-based membranes were observed by SEM for the studied time points (1, 3 and 7 days), as presented in Fig. 8.

Cell-seeded membranes showed that cells adhered to the surface of the membranes after 1 day (Fig. 8a–d), with no pronounced differences between the 4 tested conditions. Human PDLs are usually around 10–15 μm [50], which impairs their penetration across the layers of the produced electrospun mats, whose average pore size is < 5 μm. It can be observed that at day 3 (Fig. 8e–h) there was an increase in cell

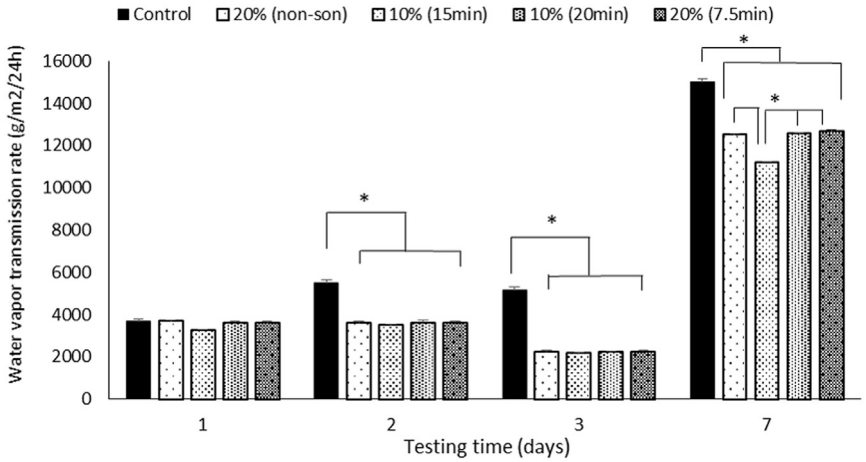

Fig. 7. Water vapor transmission rate evaluated between after 1, 2, 3 and 7 days. The asterisk (*) means that a significant statistical difference was observed between the compared samples and the control ($p < 0.05$).

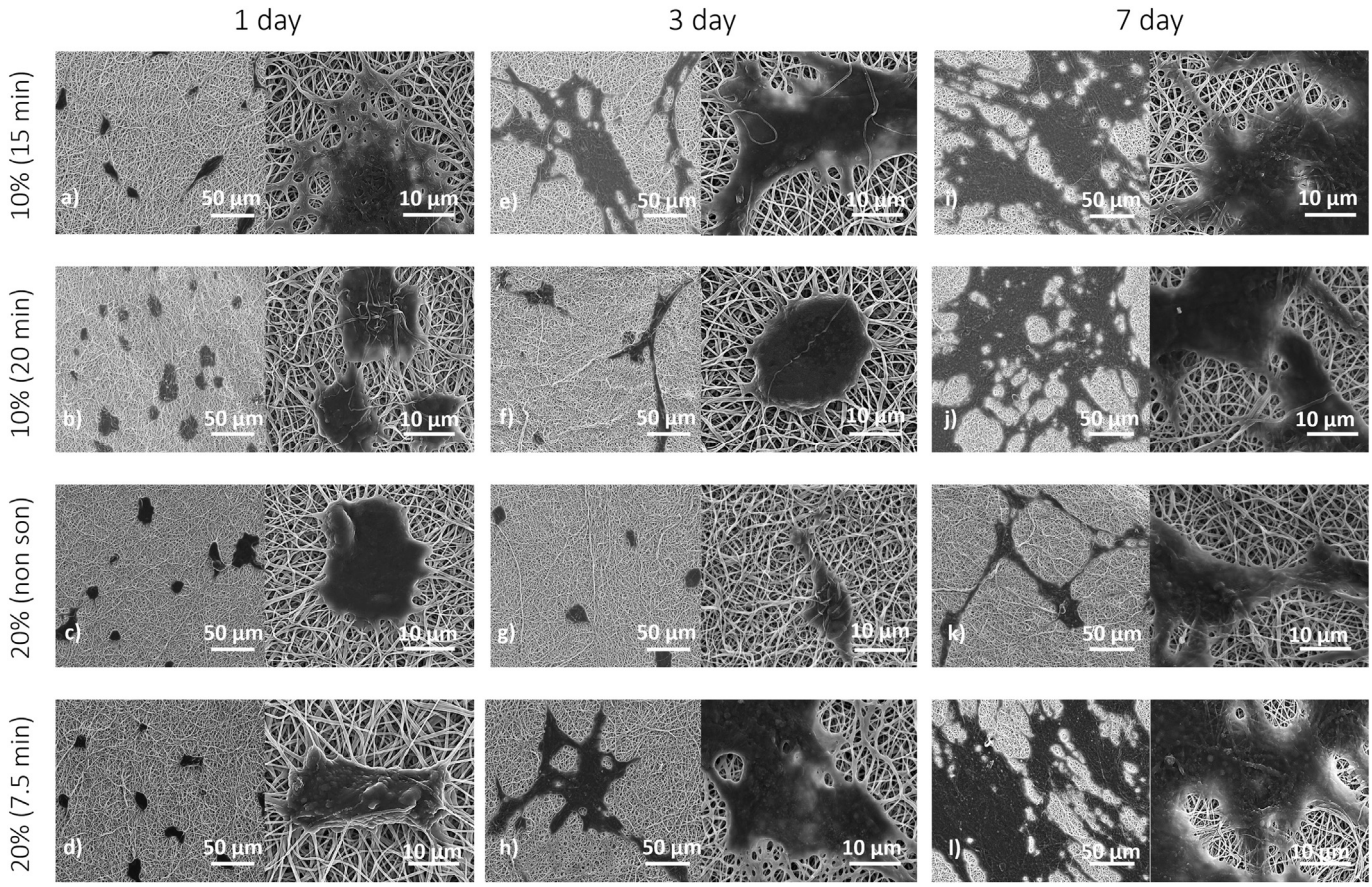

Fig. 8. SEM micrographs (500× and 2000×) of hPDLs seeded on the surface of the different electrospun matrices after 1, 3 and 7 days of culture.

density, compared to day 1 (less pronounced on 20% (non-son) formulation); it was observed that cell spread occurred and that cells were distributed and occupied a large area of the mats. At day 7 (Fig. 8i–l), the expansive behavior followed the same pattern, verified on previous days, and the cells formed a subconfluent monolayer on the surface of the membranes. Again, this behavior was not so evident on the 20% (non-son) formulation, where the cell density after 7 days of culture was visibly lower.

Confocal microscopy images obtained after Phallodin-TRITC and DAPI staining (Fig. 9) evidenced that cells presented a typical fibroblast like morphology in the silk electrospun mats, corroborating the findings obtained after SEM analysis. The formulations with the minimum amount of PEO (10%) presented more cells at the surface with time, with the cytoskeleton intensively stained in red spreading over the nanofibers. On the other hand, the formulation with the higher amount of PEO evidenced less cells at membranes' surface.

The metabolic activity and DNA quantification of human PDLs seeded and cultured onto the tested membranes after 1, 3 and 7 days of culture is presented in Fig. 10.

Cell metabolic activity increased with time for all tested membranes (Fig. 10a), which indicated that these structures are suitable for hPDLs colonization. Compared to TCPS, which is the ideal condition for cell growth, the electrospun membranes showed similar results. Regarding DNA quantification (Fig. 10b), the results are in accordance with the cell metabolic activity, where the highest amount of DNA quantification belongs to the 10% (15 min) formulation and the lowest for 20% (non-son). It is also possible to observe that DNA amount increased with time for all conditions, except the 20% (non-son). In accordance with the SEM images, cell viability and proliferation assays corroborated the increase in cell number over time in all membranes, except for the 20% (non-son), which is related with the presence of higher concentrations of PEO.

4. Discussion

4.1. Modulation of silk fibroin rheological properties by ultrasound sonication

The rheological behavior of the SF/PEO blends was observed to be PEO dependent since the increase of PEO concentration in solution led to a significant increase in viscosity. As the polymer concentration in solution increases, intermolecular distances get shorter and the interactions are favored. Initially weaker interchain interactions such as hydrogen bonds and hydrodynamic and electrostatic interactions take place, and finally the formation of β-sheet domains occurs, until a tight network is established. This effect has been previously reported [32,51,52]. Still, the objective of this study was not to focus on the PEO ability to enhance silk solutions' viscosity, but instead, to use ultrasound sonication to increase the viscosity, as a way to decrease the amount of added synthetic polymer without increasing SF concentration. The mechanical vibration during the process induces the formation and collapsing of bubbles. This physical phenomena so-called cavitation induces local heating, increase of pressure and high strain rates [36]. This method has been exploited in a variety of polymer processing applications, including self-assembly [53] and gelation [36,37]. According to the literature, it is likely that silk fibroin sol-gel transitions are influenced by the cumulative effect of several physical factors related to sonication treatment namely, mechanical/shear forces, the increase of local temperature and increased air–liquid interfaces [36].

As described in the literature, sonication physically induces a conformational transition in silk, from its primitive structure (random coil) to a β-sheet conformation (silk II structure) [37,54,55]. Wang and co-

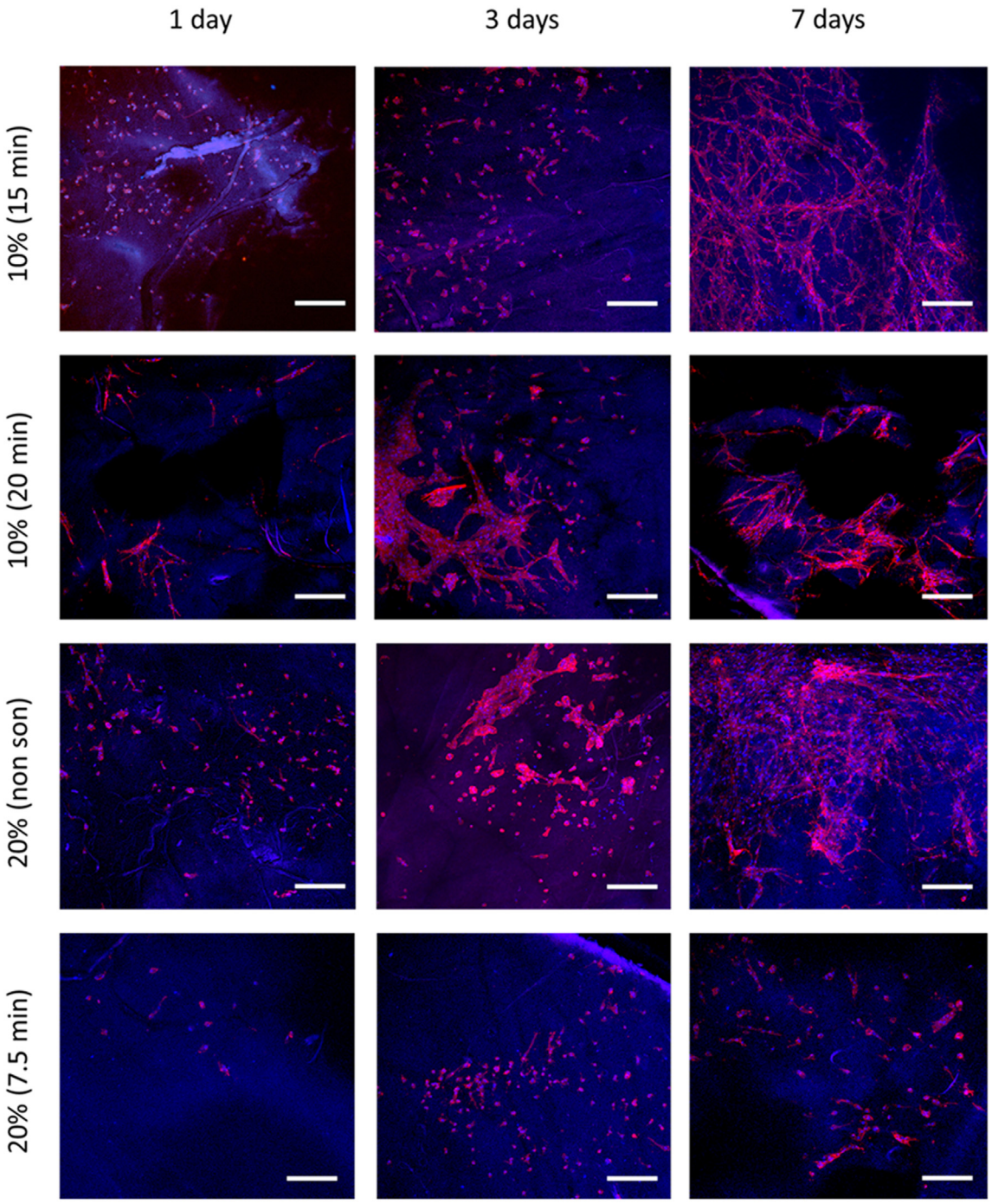

Fig. 9. Confocal microscopy of hPDLs seeded in the surface of the different electrospun matrices after 1, 3 and 7 days of culture. Cytoskeleton actin is stained in red (phalloidin-TRITC) and the nuclei are stained in blue (DAPI) (Scale bars: 200 μm). (For interpretation of the references to color in this figure legend, the reader is referred to the web version of this article.)

workers [36] demonstrated that by exposing silk fibroin to an ultrasound treatment using amplitudes of 20%, it was possible to induce the conformational transition in a controllable way, within few minutes to several hours, until jellification was observed. However, this study does not reveal the frequency used during the sonication process. According with the work of Samal et al. [37] sonication treatment induces the formation over time of a highly crystalline β-sheet conformation, due to its hydrogen bond rearrangement, followed by tight packing of stacked sheets, which serve as physical cross-links to stabilize the polymer. Therefore, when subjected to ultrasounds, SF accelerates the assembly of its hydrophobic tightening (cross-linking) and gelation occurs [37]. In the case of high molecular weight PEO (as the one used in this work), it has been reported that sonication triggers a two-step process. First, it physically breaks into low molecular weight chains, then those chains aggregate in clusters [56]. In our case, ultrasound sonication was not used as a gelling strategy but with the aim of increasing the viscosity of the solution and therefore improving the electrospinning process. A maximum of 20 min of ultrasound sonication was sufficient for allowing the formation of β-sheets without an irreversible gelling effect, which would compromise the spinnability of the solutions.

In case of solutions containing the highest amount of PEO in the blend (30%), the viscosity decreases from 15 to 20 min of sonication.

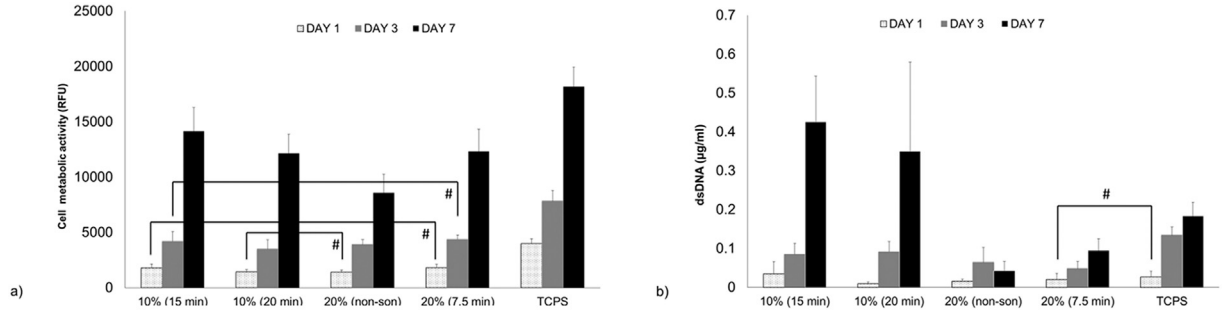

Fig. 10. a) Human PDLs metabolic activity and b) DNA quantification of hPDLs seeded in the surface of the different electrospun matrices after 1, 3 and 7 days of culture. (#) means that no significant statistical difference was found between the compared samples ($p > 0.05$).

This can possibly be explained by the occurrence of a scission of the PEO molecular chains, for being unable to dissipate the energy imposed by the sonication process, as reported by Peer et al. [57] using pure PEO solutions of concentrations up to 11%. In this case, an increase in time of sonication up to 60 min at a frequency of 24 kHz was accompanied by a progressive decrease in shear viscosity and polydispersity, being reflected in a fiber thinning. In the present study the sonication treatment up to 20 min at a frequency of 50 kHz was not reflected in a decrease in the final fiber diameter probably due to the contribution of the SF phase undergoing self-assembly. Therefore, the gelation of solutions through ultrasounds depends mostly on the polymer chemistry and its concentration, but also on sample volume, temperature, pressure, energy output (amplitude), frequency and period of sonication [36]. In the natural silkworm spinning process high shear forces are experienced at the anterior division of the silkworm gland [36]. Herein, we intend to recreate this effect first with sonication treatment and then during electrospinning, where the shear forces at the needle will induce molecular alignment and fiber formation.

4.2. Physico-chemical properties of electrospun SF/PEO nanofiber mats

Considering the increasing number of natural biocompatible polymers that have lately been emerging for membrane processing, such as collagen [17], chitosan [14,15] and gelatin [58], electrospinning was proposed as a technique with the potential to provide biodegradable nanofibrous mats, with fibers in the same order of magnitude of those present in the natural ECM structure.

Silk-based electrospun membranes have been developed in different contexts such as tissue engineered vascular grafts [23], skin tissue template/wound dressing [20], bone tissue regeneration [59] and cartilage repair [60], but have only recently been considered for dental applications. Kim et al. [59] have proposed a SF electrospun membrane for periodontal GBR, demonstrating good biocompatibility and enhancing bone regeneration in vivo, with no evidence of inflammatory reaction. However, to be electrospun, these fibers were dissolved in formic acid, which is an extremely toxic solvent, due to its inhibitory action on the mitochondrial cytochrome oxidase complex [61]. The present work silk is spun from water-based solutions. Our previous studies [62] demonstrated that the electrospinning parameters defined (30 kV of voltage, 20 µL/s of flow rate, and a plate distance of 20 cm) were not able to correctly flow silk water solutions at low concentrations (7% wt/v), forming interrupted jets of nanofibers mixed with solution's droplets, due to its low viscosity. After the dialysis process, SF solutions present a relatively low concentration, which does not allow for a stable jet formation, leading to irregular fibers with the appearance of drops. A similar effect was found by Wang et al. [63] for pure SF aqueous solutions lower than 17% (w/v). Jin et al. [32] also reported that a concentration higher than 10% (w/v) or blending with PEO (at a minimum ratio of 1:3 PEO/SF) were required to overcome the lack of electrospinnability of natural SF aqueous solutions. Huang et al. [64] and Feng Zhang et al. [51] reported that enhanced viscosities of the SF/PEO blends are directly related to the formation of a stable jet and the obtainment of a continuous and smooth fibers mesh. Usually, a higher viscosity of the fluid jet, is an indicative of a larger fiber diameter. [64] In our work the addition of PEO combined by ultrasound sonication has allowed to generate high quality silk nanofibers during electrospinning, minimizing the PEO concentration. This strategy avoids the step of concentrating the silk, which often leads to self-assembly into β-sheet conformation and consequent precipitation, simplifying the process for further scaling up.

FTIR analysis demonstrated that the SF/PEO membranes were mainly composed of random coil structures. The sonication treatment induced some degree of β-sheet conformation, as demonstrated by the analysis of the amide I region and as a consequence, the solution viscosity increased. This indicates that part of the SF structure has undergone a conformation transition, which is typically accompanied by a decrease of random coils and turns [36]. As a consequence it was possible to generate water stable membranes without the need of post-treatment using toxic solvents such as methanol.

The mechanical performance plays an important role in GTR strategies, since it is important to have a membrane adaptable and capable of physically support the regeneration of the surrounding tissues. Typically, the periodontal tissue thickness can range from 0.15 to 0.38 mm [65] and the modulus varying from 0,01 to 1750 MPa [66]. This highly variability, is due to its complex biological structure. To replace it, several membrane systems are currently in clinical use, being collagen-based decellularized membranes, the most similar to the biological tissue. However, the use of human- or animal-derived collagen encompasses regulatory issues and the risk of transmission of diseases [67]. In this work, the mechanical tests performed in the dry state to SF nanofiber membranes revealed that the highest elastic modulus, ranged between 90 MPa to 170 MPa, which is comparable with commercially available collagen based membranes, such as Jason® or Collprotect®, which present in the dry state a Young's Modulus of 178.9 and 158.5 MPa, respectively [68]. H. Cao et al. [30] reported values from 500 to 3000 MPa for electrospun regenerated SF mats of *Bombyx mori* silkworm. However, previous to electrospinning, SF solutions were concentrated to 16 wt% in a PEG solution, which adds complexity to the processing methodology. A post-spin treatment with ethanol to induce a conformational transition can also explain the higher modulus values [30]. With this hydrogen bond rearrangement crystalline stacking of the SF molecules occurs [37], increasing the modulus and the brittleness. The absence of a post-electrospinning treatment to stabilize the electrospun matrices is an important advantage of our processing strategy as compared with most of the published studies, by reducing a step and therefore simplifying the fabrication process. Despite the high stability in water, when hydrated, the mechanical performance lowers considerably. In a real scenario, we anticipate that the decrease of the mechanical properties to values in the order of those herein obtained will happen at a slower rate, due to the slower absorption of the surrounding fluids. Moreover, the membrane will be constrained by the tissue after implantation, which will help to confer some stability to it.

Further in vivo studies will be important, therefore, in order to evaluate the stability of these membranes after implantation. An effective way of increasing the mechanical properties can be to control the orientation of the fibers using specific patterns on the collector or to introduce anisotropy in the spun matrices [69].

As described in literature [70], water vapor transmission is typically evaluated in the context of skin healing and regeneration. For uncovered human dermis wounds, it's around 4800 g/m^2/24 h. The idea in this case was to use this simple method to infer about the diffusion capacity of the membranes when applied to the periodontal region. Although the obtained values appear to be higher when comparing to previous studies and with commercial polymer films [71], it is important to stress that water vapor transmission of the oral mucosa is higher than the one of the dermis, which make the membranes suitable to periodontal use.

4.3. In vitro cytotoxicity of SF/PEO nanofiber mats

Mesenchymal stem cells at the periodontal ligament are responsible for the formation and remodeling of the cementum (cementoblasts), bone (osteoblasts) and the connective tissue (fibroblasts) [72]. It has been demonstrated that SF nonwoven meshes support the adhesion, proliferation, and cell-cell interactions of a wide variety of human cell types, including epithelial cells, endothelial cells, keratinocytes, osteoblasts and fibroblasts [73]. Damrongrungruang et al. [74] verified the non-cytotoxicity of electrospun silkworm fibers by observing attachment and proliferation of gingival fibroblasts at their surface. In our study, hPDL fibroblasts were isolated and used for direct contact assays on nanofiber mats produced from different SF/PEO formulations, which were subjected to different sonication pre-treatment regimens. The results clearly demonstrated that the use of sonication pre-treatment and low amounts of PEO originated the most suitable membranes for cell studies, reflected by the improved cell adhesion, proliferation (higher DNA levels) and metabolic activity. Both SEM and confocal images showed what looks like an increase in cell density on the surface of the membranes over time, corroborated by the previous quantitative biological assays. A less favorable outcome in all biological tests was obtained for the membranes derived from the formulation using the highest content of PEO, without sonication. Jin et al. have reported a study on the response of human bone marrow stromal cells to SF/PEO nanomats, in which the presence of PEO inhibited cell adhesion in the first days of the study [35]. To overcome this effect, an additional step was introduced, to extract PEO from the mats in water for 48 h at 37 °C [35]. PEO is widely recognized as an anti-fouling material [75], which is likely to be the underlying explanation for the observed results. At low PEO concentrations, silk fibroin will have a dominant effect on the adhesion mechanisms. However, when PEO concentration is increased to 20%, its antifouling properties will have a more dominant effect, inhibiting cell adhesion, most likely via steric repulsion events [75], as succeed with our membranes.

The obtained results demonstrate that the use of controlled periods of sonication treatment offers the possibility of producing nanofiber membranes with adequate physical-chemical features and biological response. This approach cuts down the level of complexity during several processing steps and also the use of toxic solvents, which are often the cause of cytotoxicity.

5. Conclusions

The present work constitutes a step forward towards the fabrication of viable electrospun SF-based membranes for periodontal regeneration. It has been demonstrated that it is possible to tune the viscosity of SF solutions to achieve optimal processing conditions using a simple sonication step prior to the electrospinning process, as a way to render water stability, minimizing the amount of synthetic polymer without compromising the mechanical performance, expected for the envisioned periodontal application. On the other hand, lowering the amount of synthetic polymer through ultrasonication had a positive impact on the resulting biological performance, with a marked increase in cell proliferation. Silk-based materials have only recently been considered for the dental field. This work clearly demonstrates the potential of electrospun SF-based matrices for GTR in periodontal applications.

Acknowledgements

The authors acknowledge Portuguese National Funds from FCT - Fundação para a Ciência e a Tecnologia through project UID/Multi/50016/2013; Program FCT Investigator to A.L. Oliveira (IF/00411/2013), project SERICAMED (IF/00411/2013/CP1167), and through “Biotherapies-Bioengineered Therapies for Infectious Diseases and Tissue Regeneration”, funded by Norte2020. Project “IBEROS” (0245_IBEROS_1_E), funded by Fundo Europeu de Desenvolvimento Regional in the frame of Programa Interreg V A Espanha - Portugal (POCTEP) 2014–2020.

References

[1] R.C. Williams, R.J. Genco, Periodontal Disease and Overall Health: A Clinician's Guide Editors, Professional Audience Communications, Inc., Yardley, Pennsylvania, 2010.
[2] D. Joshi, T. Garg, A.K. Goyal, G. Rath, Advanced drug delivery approaches against periodontitis, Drug Deliv. 23 (2016) 1–15, https://doi.org/10.3109/10717544.2014.935531.
[3] P.I. Eke, L. Wei, G.O. Thornton-evans, L.N. Borrell, W.S. Borgnakke, R.J. Genco, Risk indicators for periodontitis in US adults: National Health and Nutrition Examination Survey (NHANES) 2009–2012, J. Periodontol. 87 (2016) 1174–1185, https://doi.org/10.1902/jop.2016.160013.
[4] M.C. Bottino, V. Thomas, G. Schmidt, Y.K. Vohra, T.M.G. Chu, M.J. Kowolik, G.M. Janowski, Recent advances in the development of GTR/GBR membranes for periodontal regeneration - a materials perspective, Dent. Mater. 28 (2012) 703–721, https://doi.org/10.1016/j.dental.2012.04.022.
[5] P.M. Bartold, S. Gronthos, S. Ivanovski, A. Fisher, D.W. Hutmacher, Tissue engineered periodontal products, J. Periodontal Res. 51 (2016) 1–15, https://doi.org/10.1111/jre.12275.
[6] S. Nyman, J. Lindhe, T. Karring, H. Rylander, New attachment following surgical treatment of human periodontal disease, J. Clin. Periodontol. 9 (1982) 290–296, https://doi.org/10.1111/j.1600-051X.1982.tb02095.x.
[7] N. Deka, Tissue engineering approach for periodontal regeneration, Int. J. Appl. Dent. Sci. 1 (2015) 71–74.
[8] H. Shimauchi, E. Nemoto, H. Ishihata, M. Shimomura, Possible functional scaffolds for periodontal regeneration, Jpn. Dent. Sci. Rev. 49 (2013) 118–130, https://doi.org/10.1016/j.jdsr.2013.05.001.
[9] S.W. Lee, S.G. Kim, Membranes for the guided bone regeneration, Maxillofac. Plast. Reconstr. Surg. 36 (2014) 239–246, https://doi.org/10.14402/jkamprs.2014.36.6.239.
[10] A.K. Singh, GTR membranes: the barriers for periodontal regeneration, DHR, Int. J. Med. Sci. 4 (2013) 31–38.
[11] Y. Rakhmatia, Y. Ayukawa, A. Furuhashi, K. Koyano, Current barrier membranes: titanium mesh and other membranes for guided bone regeneration in dental applications, J. Prosthodont. Res. 57 (2013) 12, https://doi.org/10.1016/j.jpor.2012.12.001.
[12] S. Soheilifar, S. Soheilifar, M. Bidgoli, P. Torkzaban, Barrier membrane, a device for regeneration: properties and applications, Avicenna J. Dent. Res. 6 (2014), https://doi.org/10.17795/ajdr-21343.
[13] K.A. Athanasiou, G.G. Niederauer, C.M. Agrawal, Sterilization, toxicity, biocompatibility and clinical applications of polylactic acid/polyglycolic acid copolymers, Biomaterials 17 (1996) 93–102, https://doi.org/10.1016/0142-9612(96)85754-1.
[14] C. Xu, C. Lei, L. Meng, C. Wang, Y. Song, Chitosan as a barrier membrane material in periodontal tissue regeneration, J Biomed Mater Res B Appl Biomater 100 (B) (2012) 1435–1443, https://doi.org/10.1002/jbm.b.32662.
[15] S.B. Qasim, S. Najeeb, R.M. Delaine-Smith, A. Rawlinson, I. Ur Rehman, Potential of electrospun chitosan fibers as a surface layer in functionally graded GTR membrane for periodontal regeneration, Dent. Mater. 33 (2017) 71–83, https://doi.org/10.1016/j.dental.2016.10.003.
[16] S. Zhang, Y. Huang, X. Yang, F. Mei, Q. Ma, G. Chen, S. Ryu, X. Deng, Gelatin nanofibrous membrane fabricated by electrospinning of aqueous gelatin solution for guided tissue regeneration, J. Biomed. Mater. Res. A 90 (2009) 671–679.
[17] Z. Sheikh, J. Qureshi, A.M. Alshahrani, H. Nassar, Y. Ikeda, M. Glogauer, B. Ganss, Collagen based barrier membranes for periodontal guided bone regeneration applications, Odontology 105 (2017), https://doi.org/10.1007/s10266-016-0267-0.
[18] C. Vepari, D.L. Kaplan, Silk as a biomaterial, Prog. Polym. Sci. 32 (2007) 991–1007, https://doi.org/10.1016/j.progpolymsci.2007.05.013.
[19] B.D. Lawrence, Processing of *Bombyx mori* for biomedical applications, in: S. Kundu (Ed.), Silk Biomater. Tissue Eng. Regen. Med, 1st ed., Woodhead Publishing, Cambridge, UK, 2014, pp. 78–99, , https://doi.org/10.1533/9780857097064.1.78.
[20] S.E. Wharram, X. Zhang, D.L. Kaplan, S.P. Mccarthy, Electrospun silk material

systems for wound healing, Macromol. Biosci. 103 (2010) 246–257, https://doi.org/10.1002/mabi.200900274.
[21] C. Li, C. Vepari, H.-J. Jin, H.J. Kim, D.L. Kaplan, Electrospun silk-BMP-2 scaffolds for bone tissue engineering, Biomaterials 27 (2006) 3115–3124, https://doi.org/10.1016/j.biomaterials.2006.01.022.
[22] G. Cheng, Z. Davoudi, X. Xing, X. Yu, X. Cheng, Z. Li, H. Deng, Q. Wang, Advanced silk fibroin biomaterials for cartilage regeneration, ACS Biomater. Sci. Eng. 4 (2018) 2704–2715, https://doi.org/10.1021/acsbiomaterials.8b00150.
[23] J. Zhou, C. Cao, X. Ma, J. Lin, Electrospinning of silk fibroin and collagen for vascular tissue engineering, Int. J. Biol. Macromol. 47 (2010) 514–519, https://doi.org/10.1016/j.ijbiomac.2010.07.010.
[24] M. Rajabi, M. Firouzi, Z. Hassannejad, I. Haririan, P. Zahedi, Fabrication and characterization of electrospun laminin-functionalized silk fibroin/poly (ethylene oxide) nanofibrous scaffolds for peripheral nerve regeneration, J Biomed Mater Res B Appl Biomater 106 (2017) 1595–1604, https://doi.org/10.1002/jbm.b.33968.
[25] C. Pignatelli, G. Perotto, M. Nardini, R. Cancedda, M. Mastrogiacomo, A. Athanassiou, Electrospun silk fibroin fibers for storage and controlled release of human platelet lysate, Acta Biomater. 73 (2018) 365–376, https://doi.org/10.1016/j.actbio.2018.04.025.
[26] A. Koeppel, P.R. Laity, C. Holland, Extensional flow behaviour and spinnability of native silk, Soft Matter 14 (2018) 8838–8845, https://doi.org/10.1039/c8sm01199k.
[27] J.G. Zhang, X.M. Mo, Current research on electrospinning of silk fibroin and its blends with natural and synthetic biodegradable polymers, Front. Mater. Sci. 7 (2013) 129–142, https://doi.org/10.1007/s11706-013-0206-8.
[28] Q.P. Pham, U. Sharma, A.G. Mikos, Electrospinning of polymeric nanofibers for tissue engineering applications: a review, Tissue Eng. 12 (2006) 1197–1211.
[29] H. Wang, Y. Zhang, H. Shao, X. Hu, Electrospun ultra-fine silk fibroin fibers from aqueous solutions, J. Mater. Sci. 40 (2005) 5359–5363, https://doi.org/10.1007/s10853-005-4332-2.
[30] H. Cao, X. Chen, L. Huang, Z. Shao, Electrospinning of reconstituted silk fiber from aqueous silk fibroin solution, Mater. Sci. Eng. C 29 (2009) 2270–2274, https://doi.org/10.1016/j.msec.2009.05.012.
[31] Y. Kishimoto, H. Morikawa, S. Yamanaka, Y. Tamada, Electrospinning of silk fibroin from all aqueous solution at low concentration, Mater. Sci. Eng. C 73 (2016) 498–506, https://doi.org/10.1016/j.msec.2016.12.113.
[32] H. Jin, S.V. Fridrikh, G.C. Rutledge, D.L. Kaplan, Electrospinning *Bombyx mori* silk with poly (ethylene oxide), Biomacromolecules 3 (2002) 1233–1239.
[33] M. Wang, H.-J. Jin, D.L. Kaplan, G.C. Rutledge, Mechanical properties of electrospun silk fibers, Macromolecules 37 (2004) 6856–6864, https://doi.org/10.1021/ma048988v.
[34] T. Hodgkinson, Y. Chen, A. Bayat, X.F. Yuan, Rheology and electrospinning of regenerated *Bombyx mori* silk fibroin aqueous solutions, Biomacromolecules 15 (2014) 1288–1298, https://doi.org/10.1021/bm4018319.
[35] H. Jin, J. Chen, V. Karageorgiou, G.H. Altman, D.L. Kaplan, Human bone marrow stromal cell responses on electrospun silk fibroin mats, Biomaterials 25 (2004) 1039–1047, https://doi.org/10.1016/S0142-9612(03)00609-4.
[36] X. Wang, J.A. Kluge, G.G. Leisk, D.L. Kaplan, Sonication-induced gelation of silk fibroin for cell encapsulation, Biomaterials 29 (2008) 1054–1064, https://doi.org/10.1016/j.biomaterials.2007.11.003.
[37] S.K. Samal, D.L. Kaplan, E. Chiellini, Ultrasound sonication effects on silk fibroin protein, Macromol. Mater. Eng. 298 (2013) 1201–1208, https://doi.org/10.1002/mame.201200377.
[38] L. Yan, J.M. Oliveira, A.L. Oliveira, S.G. Caridade, J.F. Mano, R.L. Reis, Macro/microporous silk fibroin scaffolds with potential for articular cartilage and meniscus tissue engineering applications, Acta Biomater. 8 (2012) 289–301, https://doi.org/10.1016/j.actbio.2011.09.037.
[39] L.J. Domigan, M. Andersson, K.A. Alberti, M. Chesler, Q. Xu, J. Johansson, A. Rising, D.L. Kaplan, Carbonic anhydrase generates a pH gradient in *Bombyx mori* silk glands, Insect Biochem. Mol. Biol. 65 (2015) 100–106, https://doi.org/10.1016/j.ibmb.2015.09.001.
[40] P. Gu, M.M. Joseph, U. Bs, R. Shiji, S. Tt, Biomedical applications of natural polymer based nanofibrous scaffolds, Int. J. Med. Nano Res. 2 (2015) 2–9.
[41] G. Rasperini, Surgical approaches based on biological objectives: GTR vs GBR techniques, Int. J. Dent. 2013 (2013) 13, , https://doi.org/10.1155/2013/521547.
[42] S.M. Yukseloglu, N. Sokmen, S. Canoglu, Biomaterial applications of silk fibroin electrospun nanofibres, Microelectron. Eng. 146 (2015) 43–47, https://doi.org/10.1016/j.mee.2015.04.008.
[43] X. Yan, S.K. Both, P. Yang, J.A. Jansen, J.J.J.P. Van Den Beucken, F. Yang, Human periodontal ligament derived progenitor cells: effect of STRO-1 cell sorting and Wnt3a treatment on cell behavior, Biomed. Res. Int. 2014 (2014) 1–10, https://doi.org/10.1155/2014/145423.
[44] K.S. Athira, P. Sanpui, K. Chatterjee, Fabrication of poly(caprolactone) nanofibers by electrospinning, J. Polym. Biopolym. Phys. Chem. 2 (2014) 62–66, https://doi.org/10.12691/jpbpc-2-4-1.
[45] X. Chen, Z. Shao, N.S. Marinkovic, L.M. Miller, P. Zhou, M.R. Chance, Conformation transition kinetics of regenerated *Bombyx mori* silk fibroin membrane monitored by time-resolved FTIR spectroscopy, Biophys. Chem. 89 (2001) 25–34, https://doi.org/10.1016/S0301-4622(00)00213-1.
[46] M. Pakravan, M.C. Heuzey, A. Ajji, A fundamental study of chitosan/PEO electrospinning, Polymer (Guildf.) 52 (2011) 4813–4824, https://doi.org/10.1016/j.polymer.2011.08.034.
[47] A.G.B. Pereira, A.T. Paulino, C.V. Nakamura, E.A. Britta, A.F. Rubira, E.C. Muniz, Effect of starch type on miscibility in poly(ethylene oxide) (PEO)/starch blends and cytotoxicity assays, Mater. Sci. Eng. C 31 (2011) 443–451, https://doi.org/10.1016/j.msec.2010.11.004.
[48] S. Suzuki, R. Dawson, T. Chirila, A. Shadforth, T. Hogerheyde, G. Edwards, D. Harkin, Treatment of silk fibroin with poly(ethylene glycol) for the enhancement of corneal epithelial cell growth, J. Funct. Biomater. 6 (2015) 345–366, https://doi.org/10.3390/jfb6020345.
[49] C.M. Muller, J.B. Laurindo, F. Yamashita, Effect of cellulose fibers addition on the mechanical properties and water vapor barrier of starch-based films, Food Hydrocoll. 23 (2009) 1328–1333, https://doi.org/10.1016/j.foodhyd.2008.09.002.
[50] S. Ivanovski, M. Komaki, P.M. Bartold, A.S. Narayanan, Periodontal-derived cells attach to cementum attachment protein via alpha5beta1 integrin, J. Periodontal Res. 34 (1999) 154–159, https://doi.org/10.1111/j.1600-0765.1999.tb02236.x.
[51] F. Zhang, B. Zuo, Z. Fan, Z. Xie, Q. Lu, X. Zhang, D.L. Kaplan, Mechanisms and control of silk-based electrospinning, Biomacromolecules 13 (2012) 798–804, https://doi.org/10.1021/bm201719s.
[52] A. Matsumoto, J. Chen, A.L. Collette, U. Kim, G.H. Altman, P. Cebe, D.L. Kaplan, Mechanisms of silk fibroin sol - gel transitions, J. Phys. Chem. B 110 (2006) 21630–21638.
[53] T. Vu, Y. Xue, T. Vuong, M. Erbe, C. Bennet, B. Palazzo, L. Popielski, N. Rodriguez, X. Hu, Comparative study of ultrasonication-induced and naturally self-assembled silk fibroin-wool keratin hydrogel biomaterials, Int. J. Mol. Sci. 17 (2016) 1–15, https://doi.org/10.3390/ijms17091497.
[54] J. Brown, C.L. Lu, J. Coburn, D.L. Kaplan, Impact of silk biomaterial structure on proteolysis, Acta Biomater. 11 (2015) 212–221, https://doi.org/10.1016/j.actbio.2014.09.013.
[55] H.-Y. Wang, Y.-Q. Zhang, Effect of regeneration of liquid silk fibroin on its structure and characterization, Soft Matter (2012) 138–145, https://doi.org/10.1039/c2sm26945g.
[56] M. Duval, E. Gross, Degradation of poly(ethylene oxide) in aqueous solutions by ultrasonic waves, Macromolecules 46 (2013) 4972–4977, https://doi.org/10.1021/ma400737g.
[57] P. Peer, P. Filip, M. Polaskova, P. Kucharczyk, V. Pavlinek, The influence of sonication of poly (ethylene oxide) solutions to the quality of resulting electrospun nanofibrous mats, Polym. Degrad. Stab. 126 (2016) 101–106, https://doi.org/10.1016/j.polymdegradstab.2016.02.002.
[58] M. Okhawilai, R. Rangkupan, S. Kanokpanont, S. Damrongsakkul, Preparation of Thai silk fibroin/gelatin electrospun fiber mats for controlled release applications, Int. J. Biol. Macromol. 46 (2010) 544–550, https://doi.org/10.1016/j.ijbiomac.2010.02.008.
[59] K. Kim, L. Jeong, H. Park, S. Shin, W. Park, S. Lee, T. Kim, Y. Park, Y. Seol, Y. Lee, Y. Ku, I. Rhyu, S. Han, C. Chung, Biological efficacy of silk fibroin nanofiber membranes for guided bone regeneration, J. Biotechnol. 120 (2005) 327–339, https://doi.org/10.1016/j.jbiotec.2005.06.033.
[60] Y. Wang, D.J. Blasioli, H.-J. Kim, H.S. Kim, D.L. Kaplan, Cartilage tissue engineering with silk scaffolds and human articular chondrocytes, Biomaterials 27 (2006) 4434–4442, https://doi.org/10.1016/j.biomaterials.2006.03.050.
[61] J. Liesivuori, H. Savolainen, H. Sciences, Methanol and formic acid toxicity: biochemical mechanisms, Pharmacol. Toxicol. 69 (1991) 157–163.
[62] R. Serôdio, S. de L. Schickert, A.R. Costa-Pinto, J. Dias, P.L. Granja, F. Yang, A.L. Oliveira, Ultrasound sonication prior electrospining tailors silk fibroin/PEO membranes for periodontal regeneration, 6th China-Europe Symp. Biomater. Regen. Med. - CESB 2017, 2017, p. 36.
[63] H. Wang, H. Shao, X. Hu, Structure of silk fibroin fibers made by an electrospinning process from a silk fibroin aqueous solution, J. Appl. Polym. Sci. 101 (2006) 961–968, https://doi.org/10.1002/app.24024.
[64] Z.M. Huang, Y.Z. Zhang, M. Kotaki, S. Ramakrishna, A review on polymer nanofibers by electrospinning and their applications in nanocomposites, Compos. Sci. Technol. 63 (2003) 2223–2253, https://doi.org/10.1016/S0266-3538(03)00178-7.
[65] A. Nanci, D.D. Bosshardt, Periodontal tissues in health and disease, Periodontol. 40 (2006), https://doi.org/10.1111/j.1600-0757.2005.00147.x.
[66] T.S. Fill, J.P. Carey, R.W. Toogood, P.W. Major, Experimentally determined mechanical properties of, and models for, the periodontal ligament: critical review of current literature, J. Dent. Biomech. 2011 (2011), https://doi.org/10.4061/2011/312980.
[67] J. Behring, R. Junker, X.F. Walboomers, B. Chessnut, J.A. Jansen, Toward guided tissue and bone regeneration: morphology, attachment, proliferation, and migration of cells cultured on collagen barrier membranes. A systematic review, Odontology 96 (2008) 1–11, https://doi.org/10.1007/s10266-008-0087-y.
[68] E. Ortolani, F. Quadrini, D. Bellisario, L. Santo, A. Polimeni, A. Santarsiero, O. George, Mechanical qualification of collagen membranes used in dentistry, Ann. Ist. Super. Sanita 51 (2015) 229–235, https://doi.org/10.4415/ANN_15_03_11.
[69] Y. B, H. Zhang, Z. Yu, H. Yuan, X. Wang, Y. Zhang, Fabrication of high performance silk fibroin fibers via stable jet electrospinning for potential use in anisotropic tissue regeneration, J. Mater. Chem. B 6 (2018) 3934–3945, https://doi.org/10.1039/C8TB00535D.
[70] Z. Gu, H. Xie, C. Huang, L. Li, X. Yu, Preparation of chitosan/silk fibroin blending membrane fixed with alginate dialdehyde for wound dressing, Int. J. Biol. Macromol. 58 (2013) 121–126, https://doi.org/10.1016/j.ijbiomac.2013.03.059.
[71] R.W. Tock, Permeabilities and Water Vapor Transmission Rates for Commercial Polymer Films, (n.d.) 223–231.
[72] J. Lindhe, N.P. Lang, T. Karring, Clinical Periodontology and Implant Dentistry Volume 1, 5th ed., Blackwell Munksgaard, Oxford, UK, 2008.
[73] H. Woo, O. Joo, J. Min, B. Mi, H. Jung, Y. Ri, M. Chae, S. Hyeon, J. Ren, C. Seok, C. Hum, Wound healing effect of electrospun silk fibroin nanomatrix in burn-model, Int. J. Biol. Macromol. 85 (2016) 29–39.
[74] T. Damrongrungruang, M. Siri-Tapetawee, S. Limmonthon, A. Rattanathongkom, Fabrication of electrospun Thai silk fibroin nanofiber and its effect on human gingival fibroblast: a preliminary study, J. Oral Tissue Eng. 5 (2007) 1–6.
[75] R.K. Bose, S. Nejati, D.R. Stu, K.K.S. Lau, Graft polymerization of anti-fouling PEO surfaces by liquid-free initiated chemical vapor deposition, Macromolecules 45 (2012) 6915–6922.